

Elsevier required licence: © <2021>. This manuscript version is made available under the CC-BY-NC-ND 4.0 license <http://creativecommons.org/licenses/by-nc-nd/4.0/>
The definitive publisher version is available online at <http://doi.org/10.1016/j.jenvman.2021.113274>

26 **Abstract**

27 Arsenic (As) is a heavy metal that causes widespread contamination and toxicity in the soil
28 environment. This article reviewed the levels of As contamination in soils worldwide, and evaluated
29 how soil properties (pH, clay mineral, organic matter, texture) and environmental conditions (ionic
30 strength, anions, bacteria) affected the adsorption of As species on soils. The application of the
31 adsorption isotherm models for estimating the adsorption capacities of As(III) and As(V) on soils was
32 assessed. The results indicated that As concentrations in contaminated soil varying significantly from
33 1 mg/kg to 116000 mg/kg, with the highest concentrations being reported in Mexico with mining
34 being the dominating source. Regarding the controlling factors of As adsorption, soil pH, clay mineral
35 and texture had demonstrated the most significant impacts. Both Langmuir and Freundlich isotherm
36 models can be well fitted with As(III) and As(V) adsorption on soils. The Langmuir adsorption
37 capacity varied in the range of 22-42400 mg/kg for As(V), which is greater than 45-8901 mg/kg for
38 As(III). The research findings have enhanced our knowledge of As contamination in soil and its
39 underlying controls, which are critical for the effective management and remediation of As-
40 contaminated soil.

41

42 *Keywords:* Arsenic; Soil contamination; Controlling factors; Adsorption isotherm; Soil remediation

43 1. Introduction

44 Arsenic (As) is a highly toxic element, and its contamination in soils, water and plants is widely
45 reported (Selim, 2012). This notorious trace metalloid has received heightened concern than other
46 heavy metals due to its toxicity and carcinogenicity to humans (Hayat et al., 2017; Jiang et al., 2017;
47 Johnston et al., 2020). Environmental problems related to As are caused by the mobilization under
48 natural conditions as well as through a range of anthropogenic sources such as mining activity,
49 combustion of fossil fuels, and use of arsenical compounds in agriculture and livestock feed
50 (Ungureanu et al., 2015). As a result, As pollution occurs widely in the environment including soil,
51 surface water (e.g., lakes, rivers), groundwater and sediment worldwide (Nguyen et al., 2019).

52 There are four valence states of As in nature including -3, 0, +3 and +5 with both organic and
53 inorganic species (Basu et al., 2014; Wang and Mulligan, 2006a). However, pentavalent arsenate
54 (As(V)) and trivalent arsenite (As(III)) are dominant among these species in natural sediment-water
55 systems (Baviskar et al., 2015). Smith et al. (2006) found that As(III) contents varied from < 5% to
56 40% of total As in railway soils in South Australia, although the source of As(III) was not provided.
57 As(V) is the most abundant form of As in oxic soil conditions ($E_h > 200$, pH 5-8) (Akter et al., 2005;
58 Álvarez-Benedí et al., 2005). The main forms of As(V) species in solution are $H_2AsO_4^-$, $HAsO_4^{2-}$ and
59 AsO_4^{3-} , while As(III) is mainly dissociated (Álvarez-Benedí et al., 2005; Martin et al., 2014) and
60 more mobile and toxic than As(V) (Akter et al., 2005). Inorganic forms of As are most volatile and
61 toxic, of which As(III) is the most toxic form being 60-100 times more toxic than As(V) (Maji et al.,
62 2007), and occurs in solution as H_3AsO_3 and $H_2AsO_3^-$. The solution pH affects the dissociation hence
63 the sorption rates of As species, with As(V) sorption decreasing while As(III) sorption increasing
64 with pH increases (Álvarez-Benedí et al., 2005; Antelo et al., 2005). Regarding the organic forms,
65 methylated species is the dominant form and may contribute substantial amounts in soils (Alloway,
66 2012). **Table 1** summarizes the structures and the acid dissociation constant (pK_a) of inorganic and
67 organic As species.

68

69 **Table 1.** Physiochemical properties of As species

Arsenic species	Dissociation reaction and structure	pK_a
Inorganic arsenate (As(V))	$H_3AsO_4 + H_2O = H_2AsO_4^- + H_3O^+$	$pK_{a1} = 2.20^a$
	$H_2AsO_4^- + H_2O = HAsO_4^{2-} + H_3O^+$	$pK_{a2} = 6.97^a$
	$HAsO_4^{2-} + H_2O = AsO_4^{3-} + H_3O^+$	$pK_{a3} = 11.53^a$
Inorganic arsenite (As(III))	$H_3AsO_3 + H_2O = H_2AsO_3^- + H_3O^+$	$pK_{a1} = 9.23^a$
	$H_2AsO_3^- + H_2O = HAsO_3^{2-} + H_3O^+$	$pK_{a2} = 12.13^a$
	$HAsO_3^{2-} + H_2O = AsO_3^{3-} + H_3O^+$	$pK_{a3} = 13.40^a$
Dimethylarsinic acid (DMA)	$As(CH_3)_2(OH)O + H_2O = As(CH_3)_2O_2^- + H_3O^+$	$pK_a = 6.20^b$
Monomethylarsonic acid (MMA)	$As(CH_3)(OH)_2O + H_2O = As(CH_3)(OH)O_2^- + H_3O^+$	$pK_{a1} = 4.10^b$
	$As(CH_3)(OH)O_2^- + H_2O = As(CH_3)O_2^{2-} + H_3O^+$	$pK_{a2} = 8.70^b$
Arsenobetaine (AsB)	$(CH_3)_3CH_2AsO_2^-$	$pK_a = 2.18^b$

70 ^a Wilson et al. (2010); ^b Reid et al. (2020)

71 Although there are several processes of As transportation in soil, adsorption is the predominant
72 process regulating As transport in aqueous systems (Stollenwerk, 2003), including the mobility, fate
73 and bioavailability (Dousova et al., 2012; Farrell, 2017; Gedik et al., 2016; Luo et al., 2019).
74 Adsorption process and its mechanisms can be well explained with different isotherm models
75 although As adsorption is greatly influenced by many factors including soil properties, As
76 concentrations, and environmental factors such as pH (Aksentijević et al., 2012; Foo and Hameed,
77 2010). Previous studies have summarized the influence of various parameters from both soil
78 properties and environmental conditions on As adsorption. For instance, Akter et al. (2005) reviewed
79 the effect of As adsorption and desorption processes on the biological availability of inorganic As
80 species in soils. Basu et al. (2014) and Smedley and Kinniburgh (2002) summarized the sources,
81 behavior, distribution, toxicity and remediation technologies of As in natural water worldwide, while
82 Smith et al. (2003) reported sources of As in natural environments and the exposure pathways in
83 Australia. Wilson et al. (2010) provided a summary of As adsorption on soils including the effects of
84 clay minerals, oxides and hydroxides, soil organic matter (SOM) as well as the adsorption
85 mechanisms. However, a critical overview of As contamination and adsorption in the soil

86 environment is still lacking, particularly in terms of the quantitative assessment of different
87 controlling factors. This article aims to provide a global assessment of As concentrations in
88 contaminated soils, to evaluate the significance of important factors affecting As adsorption behavior,
89 and to compare the modelling results from the Langmuir and Freundlich isotherms in predicting As
90 adsorption capacity and behavior in soils.

91

92 **2. As concentrations in highly contaminated soils**

93 As a result of the weathering of parent rocks, As may occur naturally in the environment, usually
94 at low concentrations (Abedi and Mojiri, 2020). Due to human activities such as medicine
95 manufacturing, metallurgical processes, and lead-acid batteries processes, the concentrations of As
96 have been increased in soils (Ong et al., 2013). The background concentration of As in natural
97 uncontaminated soils varies from 5.0 mg/kg to 7.5 mg/kg (Zhang et al., 2006) and from 42 mg/kg to
98 4530 mg/kg for polluted soils, while the average concentration of As in the earth's crust is 1.8 mg/kg
99 (Wang and Mulligan, 2006a). In comparison, the average As concentrations in soil ranged between 8
100 mg/kg and 82000 mg/kg in contaminated soils, although concentrations as high as 116000 mg/kg
101 were also reported (**Fig. 1**). The lowest mean concentrations of As (**Fig. 1**) from the soil in the United
102 States varied in the range of 0-174 mg/kg (Masri et al., 2021).

103 Although the occurrence of arsenic in the environment is a global concern, the South and East
104 Asia regions are the most severely affected (McCarty et al., 2011). For instance, in 39 soil samples
105 around an old mine in Thailand, the As concentrations varied from 4.8 mg/kg to 1070.4 mg/kg
106 (Tiankao and Chotpantararat, 2018). The concentrations of As were reported to vary at 0-6402 mg/kg
107 in agricultural soils, and at 153-294 mg/kg in mining soils from China (Jia et al., 2021). Overall, these
108 Chinese soils were considered as slightly to moderately polluted by As compared to background
109 concentration of As globally (Zhang et al., 2006), and exceeded the risk screening values in China at
110 40 mg/kg (Cao et al., 2021). The agricultural soils in Bangladesh were slightly polluted by As,
111 occurring at average As concentration of 20.3 mg/kg (**Fig. 1**).

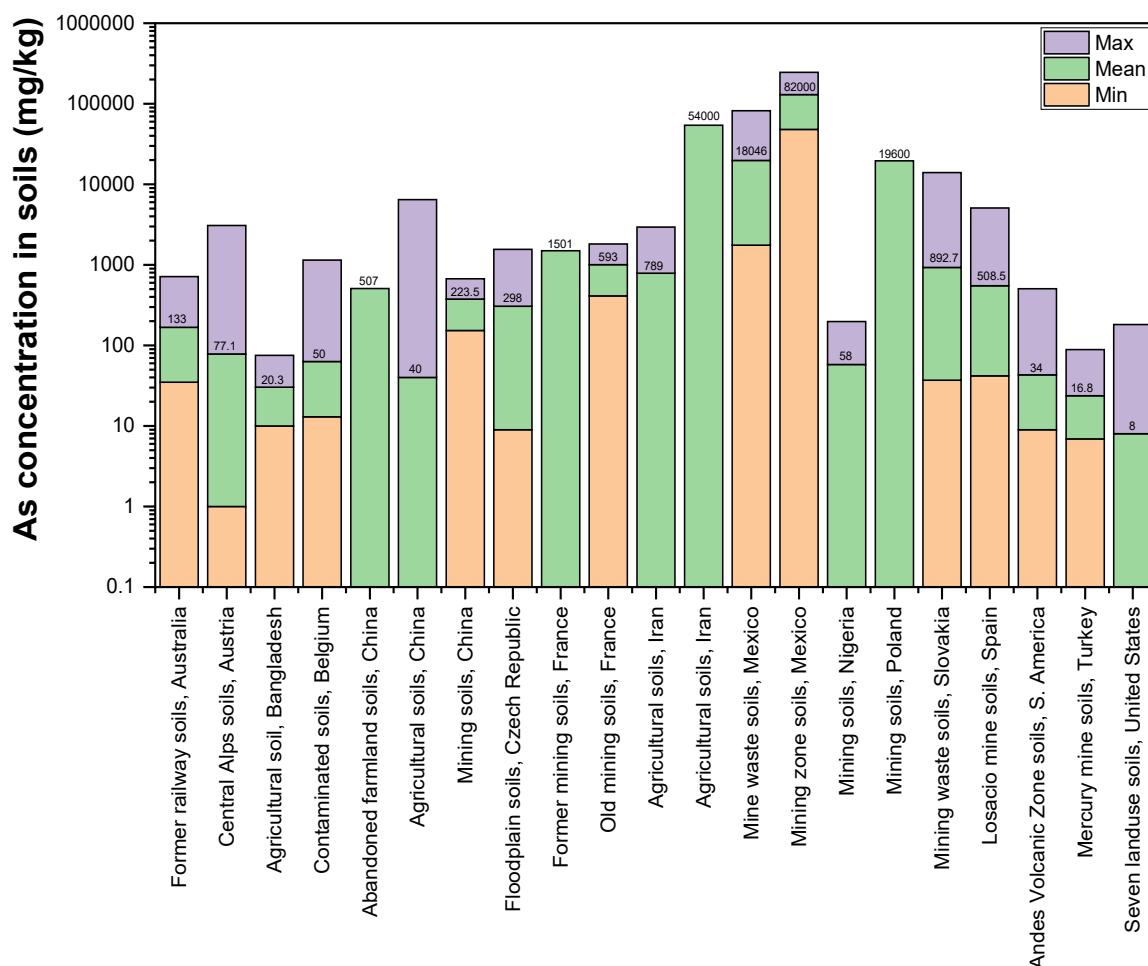
112 During the last two decades, arsenic at toxic levels has been detected in many Latin American
113 countries (Bundschuh et al., 2020). The natural activities were again found as the main sources of As
114 pollution in South America, with the mean concentration being 34 mg/kg (Tapia et al., 2019). In
115 Brazil, arsenic concentration varied from 25 mg/kg to 764 mg/kg in the shallow soils (de Figueiredo
116 et al., 2007).

117 The main source of As in the Australian soils comes from either natural or anthropogenic
118 processes. In a study in Melbourne, As concentrations ranged between <0.01 mg/kg to 27,600 mg/kg
119 (Smith et al., 2003). The repeated applications of herbicides in a large area in South Australia were
120 the reason leading to high level of As contamination in soils (35-545 mg/kg, mean = 133 mg/kg)
121 (Smith et al., 2006). The authors also reported a correlation between high concentrations of both As
122 and iron oxide content in soils ($r^2 = 0.57$), and the proportion of As(III) accounted for up to 40% of
123 the total As concentration in soils. The As concentration in the Austrian Central Alps varied in the
124 range 1-3000 mg/kg with the mean concentration of 77.1 mg/kg, which was caused by mining,
125 smelter activities and geogenic mineralization (Wenzel et al., 2002).

126 The mine soils from the European countries were reported with mean As contaminations reaching
127 over 500 mg/kg including Ouche mine soil in France (593 mg/kg), Losacio mine soil in Spain (508.5
128 mg/kg), and up to 892.7 mg/kg for Zlata Idka village in Slovakia (Rapant et al., 2006). In contrast,
129 As concentrations in soils from the Turkonu Hg mine in Turkey were low at 6.9-65.2 mg/kg, with an
130 average of 16.8 mg/kg (Gemici and Tarcan, 2007), compared to other soils polluted by mining
131 activities. The highest degree of As in contaminated soils was reported by Osuna-Martínez et al.
132 (2020), with the mean As concentrations being extremely high at 82000 mg/kg for Aurora Chihuahua
133 soils, followed by 54000 mg/kg in subsoils from Iran (Gerdelidani et al., 2021) and 18046 mg/kg in
134 Aurora mine from Mexico (Carrillo-Chavez et al., 2014) due to mining activities. Consequently,
135 different soils studied in those reports can be defined as slighted polluted by As in Bangladesh, China,
136 Czech Republic, Nigeria, South America, Turkey and United States, to moderately polluted in
137 Australia, Austria and Belgium, and highly polluted in France, Iran, Mexico, Poland, Slovakia and

138 Spain because their As concentrations all exceeded the level of uncontaminated soils at 6.0 mg/kg
 139 (Casado et al., 2007). It can also be concluded that the highest contamination of As in soils was caused
 140 by mining, followed by agricultural activities.

141



142

143 **Fig. 1.** The minimum, mean and maximum As concentrations in contaminated soil worldwide. Data
 144 from Bhuiyan et al. (2021); Cao et al. (2021); Carrillo-Chavez et al. (2014); Casado et al. (2007); de
 145 Brouwere et al. (2004); Dong et al. (2021); Gemici and Tarcan (2007); Gerdelidani et al. (2021); Jana
 146 et al. (2012); Jia et al. (2021); Kebonye et al. (2021); Lebrun et al. (2021); Masri et al. (2021); Orosun
 147 (2021); Osuna-Martínez et al. (2020); Rapant et al. (2006); Rezaei et al. (2021); Smith et al. (2006);
 148 Szopka et al. (2021); Tapia et al. (2019); Wenzel et al. (2002).

149

150 3. As adsorption by soil

151 Soils have received increasing attention as a natural sorbent in As sorption studies. The
 152 adsorption-desorption processes in soils play a key role in controlling the mobility, bioavailability,

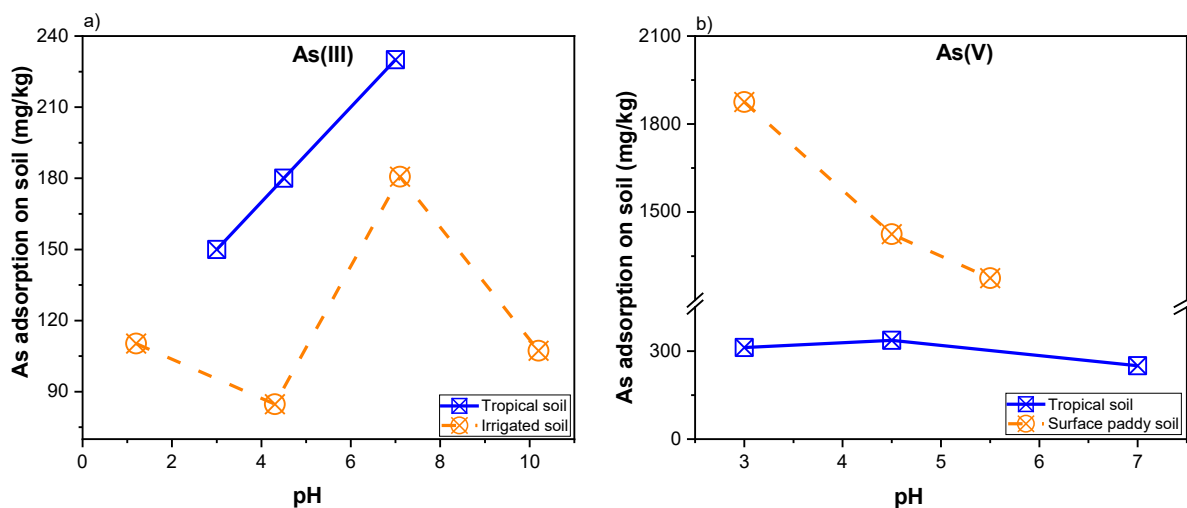
153 toxicity and fate of As in soil-water-plant systems. Soils are heterogeneous complexes of clay
154 minerals, metal oxides, organic matter and microorganisms with diverse structures (Mohapatra et al.,
155 2007), and have a high capability to adsorb metals or metalloids due to the presence of exchangeable
156 cations (e.g. Ca^{2+} , Mg^{2+} , Fe^{2+}) and anions (SO_4^{2-} , Cl^- , PO_4^{3-} , NO_3^-). Moreover, soil colloids with
157 different charges (e.g. H_2SiO_3 colloids with negative charge, $\text{Fe}(\text{OH})_3$ colloids with positive charge)
158 can affect the adsorption of arsenic on soils (Feng et al., 2013). In addition, soil properties strongly
159 affect the adsorption and desorption of As (Huling et al., 2017; Gedik et al., 2016; Selim, 2012; Xie
160 et al., 2018), while other parameters including ionic strength and competing anions (Williams et al.,
161 2003), initial concentration of As, adsorbent dose and contact time (Matouq et al., 2015), and As
162 speciation (Lomgbi and Holm, 2010) have also shown influence on As(V) adsorption.

163

164 **3.1. Soil pH**

165 Soil pH is considered as one of the most important parameters in As adsorption, and the
166 relationship between soil pH values and As adsorption has been widely investigated (Arco-Lázaro et
167 al., 2016; Campbell and Nordstrom, 2014). The important role of pH in As adsorbed on soils is due
168 to its effect on As speciation and the charge of soil particle surfaces (Gitari and Mudzielwana, 2018;
169 Huang et al., 2013). As(V) adsorption decreased significantly while As(III) adsorption increased on
170 soils with the pH increase (Álvarez-Benedí et al., 2005; Deng et al., 2018; Fan et al., 2020). As(V)
171 adsorption is extremely dependent on pH values (Williams et al., 2003), and the increase in pH can
172 cause an increase in repulsion of the soil surface to arsenate, resulting in the decrease in arsenate
173 adsorption (Jiang et al., 2017). On the other hand, As(III) adsorption was highly favored on positively
174 charge sites in soil through electrostatic attraction under the acidic condition (Renkou et al., 2009).
175 Goldberg et al. (2005) suggested that As(V) adsorption exhibited a maximum in adsorption around
176 pH 6-7, and then decreased with further increase in solution pH. A study on the adsorption-desorption
177 of As(V) in three Spanish soils showed that pH values slightly reduced during the As adsorption
178 experiments and pH was more important on As(V) sorption at high concentrations and for variations

179 of several pH units (Álvarez-Benedí et al., 2005). **Fig. 2a** illustrates that the maximum adsorption of
 180 As(III) on a tropical soil increased from 150 mg/kg to 230 mg/kg when pH was increased from 3 to
 181 7 (Goh and Lim, 2004), and reached the peak of 180.8 mg/kg at pH 7.09 for irrigated soil (Huang et
 182 al., 2013). In contrast, the adsorption of As(V) on surface paddy soil (Jiang et al., 2017) decreased
 183 from 1875 mg/kg (pH 3) to 1275 mg/kg (pH 5.5), or reached the maximum of 337 mg/kg at pH 4.5
 184 for tropical soil (**Fig. 2b**). The fact that soil surface positive charge density decreased with the increase
 185 in pH of the system could be due to the increasing amount of the OH⁻ ions, resulting in decreasing
 186 adsorption (Goh and Lim, 2004). Moreover, Jeppu and Clement (2012) successfully incorporated
 187 sand pH value as a dependent variable of the modified Langmuir-Freundlich (MLF) isotherm
 188 equation for predicting As(V) adsorption onto pure goethite and goethite-coated sand sorbents. On
 189 the other hand, pH may not be considered as a main factor affecting As sorption capacities (Alloway,
 190 2013), and the effects of soil pH on As adsorption were difficult to conclude (Jiang et al., 2005b).
 191 The adsorption capacity of As(V) on iron ore reached a maximum of 400 mg/kg at pH 4.5-6.5 (Zhang
 192 et al., 2004). Although Alloway (2013) suggested that the effect of pH on As(V) adsorption was
 193 generally small, the data from the previous investigations (**Figs 2a** and **2b**) indicated that soil pH had
 194 significant effects on the adsorption of both As(III) and As(V) on soil.



195
 196 **Fig. 2.** Effects of pH on (a) As(III) adsorption on a tropical soil (Goh and Lim, 2004) and an irrigated
 197 soil (Huang et al., 2013); b) As(V) adsorption on a tropical soil (Goh and Lim, 2004) and a surface
 198 paddy soil (Jiang et al., 2017).

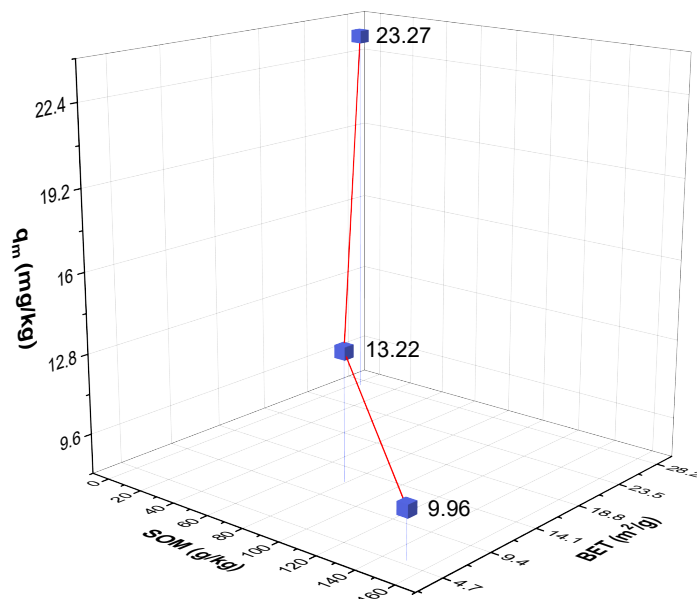
199

200 3.2. Clay minerals

201 Clay minerals have a significant influence on As sorption in soils due to their unique
202 physicochemical properties such as chemical and mechanical stability, large specific surface area,
203 high charge density, layered structure and high cation exchange capacity (Gitari and Mudzielwana,
204 2018; Mukhopadhyay et al., 2017). The large total surface area is one essential property of clay
205 minerals (Gitari and Mudzielwana, 2018) which represents the sum of external surface area and the
206 internal surface area corresponding to the interlayer spaces (Jlassi et al., 2017), which allows clay
207 minerals to adsorb water and environmental contaminants. Macht et al. (2011) expressed that the
208 specific surface area of natural particles plays an important role in quantifying sorptive process in
209 soils. For example, the adsorption capacities of total As on three soils increased with an increase of
210 soil surface area (**Fig. 3**). Similarly, Xie et al. (2018) found that the adsorption capacity of As(III) and
211 As(V) decreased with the reduction of soil clay content, with S3 (45.5% clay) > S2 (11.0% clay) >
212 S1 (7.2% clay), as shown in **Fig. 4**. The role of clay content would enhance As(V) adsorption on the
213 low-energy surface because the behavior of As on clay minerals is similar to that on the oxides
214 (Goldberg, 2002), and large surface areas and active sites of clay minerals would provide a high
215 capacity for As adsorption (Jiang et al., 2005b; Foroutan et al., 2019). Foroutan et al. (2019) reported
216 the highest adsorption of As(V) on natural clay (~94%) at pH 3-4, which decreased to under 30%
217 when pH was 9.0; the results were explained by the interactions between negative hydroxyl ions with
218 As(V) ions in aqueous solution. According to Gitari and Mudzielwana (2018), the adsorption of
219 As(III) was via physisorption and occurred on the outer layer surface complex of the adsorbent while
220 the adsorption of As(V) was via chemisorption and occurred in the inner layer surface complex of the
221 adsorbent.

222 The reaction of physical adsorption occurs rapidly on the surface of adsorbents with low enthalpy
223 and creating multilayer formation. In contrast, chemical adsorption reacts slowly and irreversibly,
224 having high enthalpy and monolayer formation. Similarly, Fan et al. (2020) suggested that sharing or
225 exchange of electrons between adsorbent and adsorbate was involved in the chemisorption process

226 of As(V) adsorbed on the black soil. Therefore, As adsorption will be favored in terms of clay
227 minerals in soils (Arco-Lázaro et al., 2016).



228

229 **Fig. 3.** Effects of the surface area of clay minerals and SOM on the adsorption of total As on soils
230 (Feng et al., 2013).

231 3.3. SOM

232 SOM plays a major role in enhancing the release of As from soils to the solution (Wang and
233 Mulligan, 2006a). SOM is derived from the decomposition of terrestrial and aquatic animals and
234 plants that strongly interacts with As and affects its species and mobility in aquatic environments
235 (Wang and Mulligan, 2006a). Varsányi and Kovács (2006) suggested that there was a correlation
236 between total As and particulate organic carbon with low contents of extracted Fe (4.91 g/kg) and
237 organic carbon in soil (0.04%), while no correlation was observed with higher concentration of
238 extracted Fe (7.75 g/kg) and organic carbon content (0.09%). Jiang et al. (2005b) found that dissolved
239 SOM reduced As(V) adsorption on both high- and low-energy surfaces of soil adsorption sites. It is
240 postulated that dissolved organic matter competed with As for adsorption to mineral surfaces or
241 formed complexes with As(V); however, the percentage of As retention on natural organic matter
242 was low (Wilson et al., 2010). Grafe et al. (2001) suggested that high stability of As in ionic solutions

243 was due to the prevented aggregation of organic matter leading to the balanced distribution of surface
244 charge, and expressed that As(V) released from soils was controlled by organic matter regardless of
245 the adsorption mechanism. Similarly, Feng et al. (2013) and Wang and Mulligan (2006b) pointed out
246 that SOM had great potential effects on As adsorption behavior due to its interactions with mineral
247 surfaces and/or with As itself. **Fig. 3** shows that the maximum adsorption capacity (q_m) from the
248 Langmuir isotherm model of total As on three Chinese soils increased with a decrease in SOM. It was
249 suggested that a portion of As was bound to SOM (humic acids) through positively charged amine
250 groups (Varsányi and Kovács, 2006), resulting in the negative impact of SOM on As adsorption on
251 soils (Huang et al., 2013).

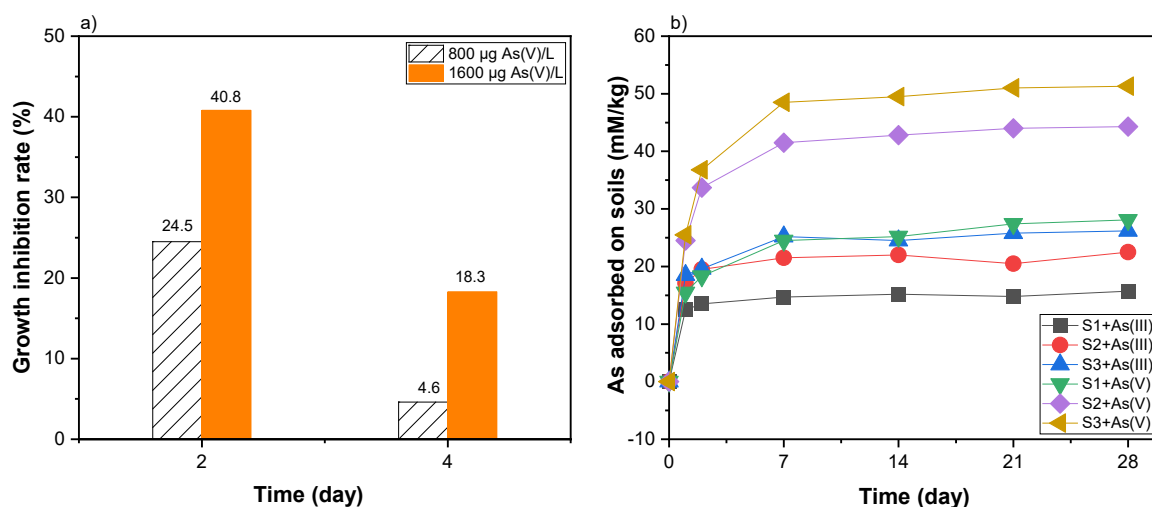
252

253 **3.4. Bacteria**

254 Bacteria can affect As adsorption because they can resist As(V) toxicity by reducing intracellular
255 As(V) to As(III) (Wang and Mulligan, 2006b). Campbell and Nordstrom (2014) stated that microbial
256 redox cycling plays a role in accelerating the kinetics of As(III) oxidizing or As(V) reducing reactions,
257 which affect the speciation of As in the environment. Furthermore, Wang and Mulligan (2006b)
258 suggested As(V) can be used as an electron acceptor of anaerobic microorganisms for the oxidation of
259 organic matter or H₂ gas. Xie et al. (2013) found that the rate of growth inhibition of bacteria increased
260 with the increasing initial As(V) solution during 4-day reaction time (**Fig. 4a**). They found that the
261 highest inhibition rates occurred on the second day of exposure, being 24.5% and 40.8% with As(V)
262 concentration of 800 µg/L and 1600 µg/L, respectively, which gradually decreased to 4.6% and 18.3%
263 at the end of reaction (**Fig. 4a**). The authors suggested that the presence of As(V) significantly
264 affected the growth of bacterial cells till the second day of exposure, and then most of the organisms
265 had been adapted to the As(V) stress environment, resulting in a decrease in the growth inhibition
266 rates to their lowest levels (Xie et al., 2013).

267 In turn, the presence of bacteria influenced the adsorption of As on soil particles. As shown in
268 **Fig. 4b**, the adsorption occurred rapidly during the first 7-days, and then gradually increased at the

269 end of exposure. For instance, the estimated As(III) concentrations in these three soils were 12.5
 270 mmol/kg, 17.1 mmol/kg and 18.5 mmol/kg at the first day, and reached 15.7 mmol/kg, 22.5 mmol/kg
 271 and 26.2 mmol/kg at 28 days for S1, S2 and S3, respectively. The results for As(V) were 15.5
 272 mmol/kg, 24.5 mmol/kg and 25.5 mmol/kg at the first day, and 28.1 mmol/kg, 44.3 mmol/kg and
 273 51.3 mmol/kg at 28 days for S1, S2 and S3, respectively. It can also be found that the amounts of
 274 As(III) and As(V) adsorption on S3 were significantly higher than those of S1 and S2 at any exposure
 275 time, which were attributed to the fact that S3 contained higher amount of clay (45.5%) and Fe₂O₃
 276 (4.68%) than S1 with 7.2% clay and 3.16% Fe₂O₃, and S2 with 11.0% clay and 3.95% Fe₂O₃. These
 277 soil properties can enhance the adsorption of As on soil. Xie et al. (2013) suggested that bacteria can
 278 change their shape, activate detoxifying processes and strengthen antioxidant defense systems in order
 279 to adapt to an environment with high As contamination. It can be concluded that bacteria could reduce
 280 the adsorption affinity of As on soils because As(V) could be reduced to As(III) under the impact of
 281 bacteria, then As(III) was released from solid phase into solution (Xie et al., 2018).



282 **Fig. 4.** Interactions between bacteria and As adsorption. A) Effect of As(V) on the growth inhibition
 283 rate of bacteria (Xie et al., 2013); b) effect of bacteria on As(V) and As(III) adsorption on different soils
 284 during 28-day of exposure, modified from the results of Xie et al. (2018).

286 3.5. Ionic strength

287 The effect of ionic strength on As sorption on soils varied between As(V) and As(III). The
 288 adsorption of As(V) ions increased with ionic strength at pH > 5.0, but was not significantly affected

289 by ionic strength at $\text{pH} < 5.0$ (Antelo et al., 2015). In contrast, ionic strength had a relatively small
 290 effect on As adsorption (Williams et al., 2003). Renkou et al. (2009) showed that increasing ionic
 291 strengths resulted in higher As(V) adsorption and lower As(III) adsorption on the two soils
 292 investigated under acidic condition, whilst the amount of adsorbed As(III) increased with increasing
 293 solution pH. Antelo et al. (2015) reported that As(V) adsorption on ferrihydrite was influenced by the
 294 presence of Ca^{2+} ions at relatively high pH values (> 8) while not influenced at $\text{pH} < 8.0$ due to the
 295 weak adsorption of Ca^{2+} . The rate of As(V) adsorption increased by up to 30% when the concentration
 296 of Ca^{2+} was increased from 0.3 mM to 6.0 mM at pH 10.2. As shown in **Fig. 5a**, Smith et al. (2002)
 297 compared the effects of Ca^{2+} and Na^+ on As(III) and As(V) adsorbed onto Alfisol soil, with Ca^{2+}
 298 having a greater influence on the adsorption of both As(III) and As(V) than Na^+ . For example, the
 299 maximum adsorption of As(III) and As(V) in the presence of 0.1 mmol $\text{Ca}(\text{NO}_3)_2$ was 0.50 mmol/kg
 300 and 1.85 mmol/kg, higher than 0.40 mmol/kg and 1.30 mmol/kg in the presence of 0.1 mmol NaNO_3 ,
 301 respectively. In addition, the results showed that the adsorption of As(V) was significantly higher
 302 than that of As(III) (**Fig. 5b**). In general, the ionic strength had a marginally positive effect on As
 303 sorption on soils during both physisorption and chemisorption.

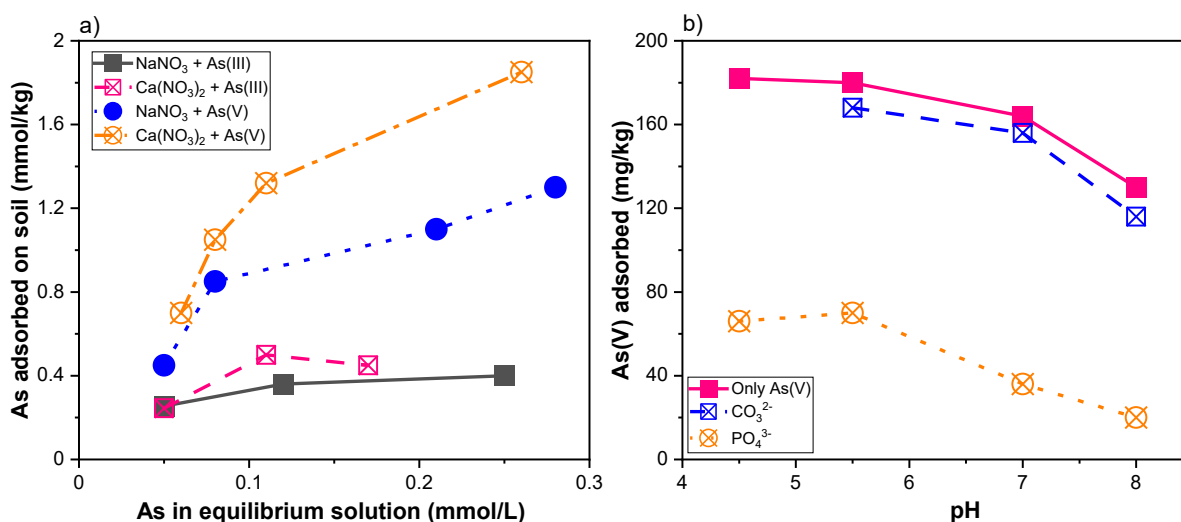


Fig. 5. a) Effects of Na^+ and Ca^{2+} on As(III) and As(V) adsorption on soil (Smith et al., 2002); b) effects of anion competition from CO_3^{2-} and PO_4^{3-} on As(V) adsorption on soil (Williams et al., 2003).

304

305 **3.6. Anion competition**

306 As adsorption generally decreased with the presence of anion competition (Alloway, 2013).
307 Sharing the same chemical characteristics, the presence of PO_4^{3-} ions significantly decreased the
308 adsorption of As(V) through the competitive adsorption of As(V) and PO_4^{3-} on minerals and soils
309 (Selim, 2012; Williams et al., 2003) due to the positively-charged surface of soils and iron oxides
310 (Jiang et al., 2017). As(V) adsorption on bulk soils greatly decreased within the pH 3.0-4.5 with the
311 presence of phosphate (Jiang et al., 2017). Similar effect of phosphate on As(III) sorption was found
312 on the Alfisol and Oxisol soils in Australia (Smith et al., 2002), in which the amount of As(III)
313 adsorption in soil decreased from 0.38 mmol/kg to 0.1 mmol/kg at an equilibrium As(III)
314 concentration of 0.2 mmol/L in the presence of phosphate in solution. The effect of phosphate on As
315 adsorption varied in different soils. For example, at 12.0 $\mu\text{g/L}$ As concentration, the adsorption of
316 As(V) and As(III) on soil from Beijing was 1.75 mg/kg and 1.16 mg/kg in the absence of phosphate,
317 which was reduced to 0.75 mg/kg and 0.33 mg/kg in the presence of phosphate, respectively (Feng
318 et al., 2013). Zhang et al. (2004) found that the presence of phosphate had a significantly negative
319 effect on As adsorption while sulphate and chloride contents slightly enhanced the adsorption.
320 However, the concentration of PO_4^{3-} exhibited less effect on both As(V) and As(III) adsorption on
321 soil from Hainan, China (Feng et al., 2013). Other anions presenting in soil solutions at higher
322 concentrations such as CO_3^{2-} , Cl^- , SO_4^{2-} and NO_3^- had a relatively small effect on As(V) adsorption
323 (Álvarez-Benedí et al., 2005; Huang 2018; Williams et al., 2003). **Fig. 5b** compared the effects of
324 CO_3^{2-} and PO_4^{3-} due to the anion competition for As(V) adsorption onto soil (Williams et al., 2003).
325 Of different anions, it was found that CO_3^{2-} slightly reduced the adsorption of As(V) on soil at
326 different pH values, while PO_4^{3-} had significantly reduced As(V) adsorption by 110-128 mg/kg at pH
327 4.5-8.0. Such results were explained by Welch and Stollenwerk (2003) as due to sulphate adsorbed
328 via electrostatic attraction acting as an outer-sphere complex in the presence of net positive surface
329 charge on soil. As a result, phosphate ions have shown strongly negative effects on As(III) and As(V)

330 adsorption (Zeng et al., 2012) via chemisorption while other anions reduce As adsorption through
331 physisorption.

332

333 **3.7. Initial As concentration, adsorbent dose and contact time**

334 The initial concentration of arsenic in solution, adsorbent dose and contact time are considered
335 as important parameters influencing the adsorption of As (Matouq et al., 2015). In general, increasing
336 initial concentration of As(V) or As(III) in solution leads to high rate of adsorption (Wang et al.,
337 2018). The adsorption of As(V) on sediment in Wuhan, China was higher than that of As(III) at high
338 initial As concentrations, particularly below 3.33 $\mu\text{mol/L}$ As (Wang et al., 2018). However, Yolcubal
339 and Akyol (2008) observed the opposite results that the degree of As(V) sorption in carbonate-rich
340 soils at equilibrium in batch experiments decreased with increase in As(V) concentrations (0.1–200
341 mg/L). Regarding adsorbent dose, the adsorption efficiency of natural clay and clay/Fe-Mn composite
342 for As(V) rapidly increased from 41.32% to 94.76% and from 47.27% to 98.82% with adsorbent
343 concentration increasing from 0.25 to 2.0 g/L, respectively (Foroutan et al., 2019), although the
344 adsorption efficiency did not show significant changes when the adsorbent dose was higher than 1.5
345 g/L. In addition, Zhang et al. (2004) found that the residual As(V) concentration decreased from 1.0
346 mg/L to below detection limit when the amount of adsorbent (iron ore) was increased from 0 to 5.0
347 g/L.

348 The adsorption of As from batch experiments displayed a strong time-dependent kinetic behavior
349 (Selim, 2012). Adsorption process exhibited a rapid rate at the initial stage, e.g. within the first 24 h
350 (Guo et al., 2007; Zhang et al., 2004), 48 h (Williams et al., 2003) or seven days (Xie et al., 2018),
351 followed by a slower or stable rate over the next several weeks (Williams et al., 2003). Based on the
352 laboratory batch experiments, As adsorption reached 99.0% and 98.7% for soils from Beijing and
353 Hainan, but only 34.0% for soils from Jilin, China after two hours of reaction during which the
354 adsorption capacities of As(V) and As(III) reached 386 mg/kg and 458 mg/kg with a contact time of
355 194 h (Guo et al., 2007; Feng et al., 2013). The adsorption amount of As(III) on irrigated soils

356 achieved 33% within the first hour of contact, with further adsorption of 9.4% in the following 23 h
357 (Huang et al., 2013).

358

359 **3.8. Soil texture**

360 Guo et al. (2007) reported that As adsorption on the fine grains (0.10-0.25 mm) of natural siderite
361 was higher than on the coarse ones due to their greater surface areas. A study by Álvarez-Benedí et
362 al. (2005) showed that the amount of As adsorbed in the sandy clay loam soil with a large surface
363 area was significantly higher than in the loamy sand soil. In addition, the grain size influenced the
364 adsorption of As species (Guo et al., 2007). For instance, greater As(III) adsorption occurred with the
365 grain size fractions of 0.04-0.08 mm and 0.25-0.50 mm than that of As(V) while the opposite trend
366 happened with the grain size fraction of < 0.04 mm. According to Xie et al. (2018), the adsorption
367 capacity decreased in accordance with particulate texture, i.e. clay loam > loamy sand > silty sand
368 and was higher for As(V) than for As(III) in the presence of bacterial activity. Smith et al. (2006)
369 reported that As concentrations on soils from South Australia decreased from 256-1389 mg/kg on clay
370 fraction (0-2 µm) to 170-675 mg/kg on sand fraction (250-2000 µm). However, Jiang et al. (2005a;
371 2005b) did not observe any relationship between the changes of clay contents and As(V) adsorption
372 when they studied the adsorption of As(V) on 16 soils in China. In addition, there was no significant
373 correlation between the proportion of particulate grain size and total As content in the study of
374 Varsányi and Kovács (2006). However, Smith et al. (2006) reported that the total As concentrations
375 increased markedly with decreasing particle size as sand < silt < clay, with increasing As
376 concentration generally correlated with increasing Fe concentrations ($r^2 = 0.57$). Hence, a high
377 proportion of clay fraction would enhance the adsorption of As on soils.

378

379 **3.9. As speciation**

380 The adsorption rates of As are influenced by its speciation, with faster rate of As(V) adsorption
381 than that of As(III) at low pH, and slower and similar rate to As(III) adsorption at high pH 9 being

382 reported (Welch and Stollenwerk, 2003). The adsorption of As(V) on Olivier loam and Windsor sand
383 soils was higher than As(III) adsorption under varying conditions of As concentration, pH, and ionic
384 strength (Mohan and Pittman, 2007). The adsorption of As(V) on tropical soils and goethite was
385 stronger than that of As(III) (Goh and Lim, 2004; Huang, 2018), who reported that the percentages
386 of As(V) and As(III) adsorbed on the tropical soil increased from 83% and 50% after 8 h to 92% and
387 58% at 24 h, respectively. Regarding As species, the concentrations of As(III) and As(V) were highly
388 dependent on pH and redox conditions (Eh) in soil and water (Wang and Mulligan, 2006b). As(V) is
389 dominating under oxic conditions (Eh > 200 mV, pH 5-8) (Violante and Pigna, 2002), while As(III)
390 mainly occurs in reducing conditions (Wang and Mulligan, 2006a). As(V) reserves its stable redox
391 state under oxidizing conditions in soils (Goldberg et al., 2005), and as a result, As(V) species has
392 been widely investigated in adsorption on soils (Álvarez-Benedí et al., 2005; Arco-Lázaro et al., 2016;
393 Fan et al., 2020; Farrell 2017; Gedik et al., 2016; Goldberg and Suarez, 2013; Gustafsson, 2006; Jiang
394 et al., 2005a, b; Jiang et al., 2017; Luo et al., 2019; Williams et al., 2003; Yolcubal and Akyol, 2008;
395 Zhang and Selim, 2005). Both As(III) and As(V) have been studied to evaluate the adsorption-
396 desorption mechanisms under different controlling factors (Deng et al., 2018; Dousova et al., 2012;
397 Feng et al., 2013; Guo et al., 2007; Mishra and Ramaprabhu, 2012; Qiu et al., 2018; Renkou et al.,
398 2009; Wang et al., 2018), although only a few studies focused on As(III) sorption (Caporale et al.,
399 2013; Huang et al., 2013). The mechanism for contaminant adsorption by a solid surface can be used
400 to explain the difference of As speciation adsorbed on soils. There are three common adsorption
401 mechanisms including outer-sphere surface complexation, physisorption inner-sphere complexation,
402 and chemisorption (Welch and Stollenwerk, 2003). The complex bonds of inner-sphere are stronger
403 than those of outer-sphere because the electrostatic attraction between a charged surface and an
404 oppositely charged ion in solution involved in outer-sphere is weaker than the formation of a
405 coordinative complex with the mineral surface involved in inner-sphere. Consequently, As(V)
406 adsorption on soil via chemisorption is stronger than As(III) adsorption via physisorption (Ma et al.,
407 2015). The results (**Fig. 6**) illustrate that As(V) adsorption was higher than As(III), which agree with

408 the results from Fendorf et al. (2010).

409

410 **3.10. Bioavailability of As in soils**

411 Bioavailability of As is dependent on several factors including soil properties, adsorption and
412 desorption processes, plant species and microbial processes (Akter et al., 2005). The soil factors
413 include clay content, SOM, texture, pH, Eh, cation exchange capacity, oxides and hydroxides of Fe,
414 Al and Mn (Akter et al., 2005). According to Yang et al. (2002), Fe oxide content and pH were the
415 most important soil properties influencing the bioavailability of As on aging. They reported that high
416 Fe oxide content and low pH (< 6) significantly reduced As bio-accessibility over 6 months, while
417 As could become more bioavailable with soil pH > 6. The study also found that the mean initial bio-
418 accessibility of As(V) in 36 soils was 43.6% at the beginning of adsorption, then reduced marginally
419 to 40.1%, 36.5%, 35.6% and 33.0% after 1, 2, 3 and 6 months, respectively. Adsorption process is
420 also able to reduce the mobility and bioavailability of As in soils. For instance, As(III) was more
421 bioavailable than As(V) at higher pH due to stronger adsorption affinity of As(V) on metal oxides,
422 especially Fe oxides (Akter et al., 2005). Plant species are generally able to accumulate part of As
423 concentrations in soils to their root and translocate to shoot and grains (Neidhardt et al., 2015). The
424 amount of As accumulation depends on the accumulation and translocation ability of the plants
425 (Huang et al., 2006). The uptake mechanisms of As(III) and As(V) occur in different ways. For
426 example, rice plants can accumulate As(III) in their shoots through silicon uptake pathway (Fleck et
427 al., 2013), while plants uptake of As(V) is through phosphate transport channels (Bhattacharya et al.,
428 2021). As(III) can be removed by microorganisms such as bacteria, fungi and algae which can reduce
429 As(V) to As(III) (Akter et al., 2005) and release As(III) from soil to solution (Xie et al., 2018),
430 resulting in less bioavailability of As in soils as long as there is no limitation to soil drainage. Hence,
431 As(III) is more mobile while As(V) is more bioavailable in soils due to its negative charge and
432 stronger retention in soils (Lombi and Holm, 2010).

433 Therefore, As adsorption is highly dependent on soil properties such as pH, texture, clay minerals

434 and environmental factors namely initial As solution, sorbent dose and reaction time (Huang et al.,
435 2013). Dias et al. (2009) suggested that iron oxide content was the most important soil parameter
436 affecting As(III) adsorption on soils, while soil textures including sand, silt and clay fractions were
437 the most important factors for As(V) adsorption on soils.

438

439 **4. As adsorption isotherm models**

440 The Langmuir and Freundlich isotherm models have been widely applied for As sorption as these
441 models can provide a good fit of results under a range of different conditions. According to Ghosal
442 and Gupta (2017), the Langmuir isotherm is most applicable for the chemisorption process since it is
443 primarily used for unimolecular adsorption with the assumption of monolayer surface coverage,
444 independent and homogeneous sorption and energy, whilst the Freundlich isotherm exhibits the
445 physical adsorption which was developed for the heterogeneous surface with non-uniform
446 distribution of adsorption heat and unrestricted monolayer coverage.

447 **4.1. The Langmuir isotherm model**

448 The Langmuir adsorption isotherm is expressed in Eq. (1) (Matouq et al., 2015):

$$449 \quad q_e = \frac{K_L q_m C_e}{1 + K_L C_e} \quad (1)$$

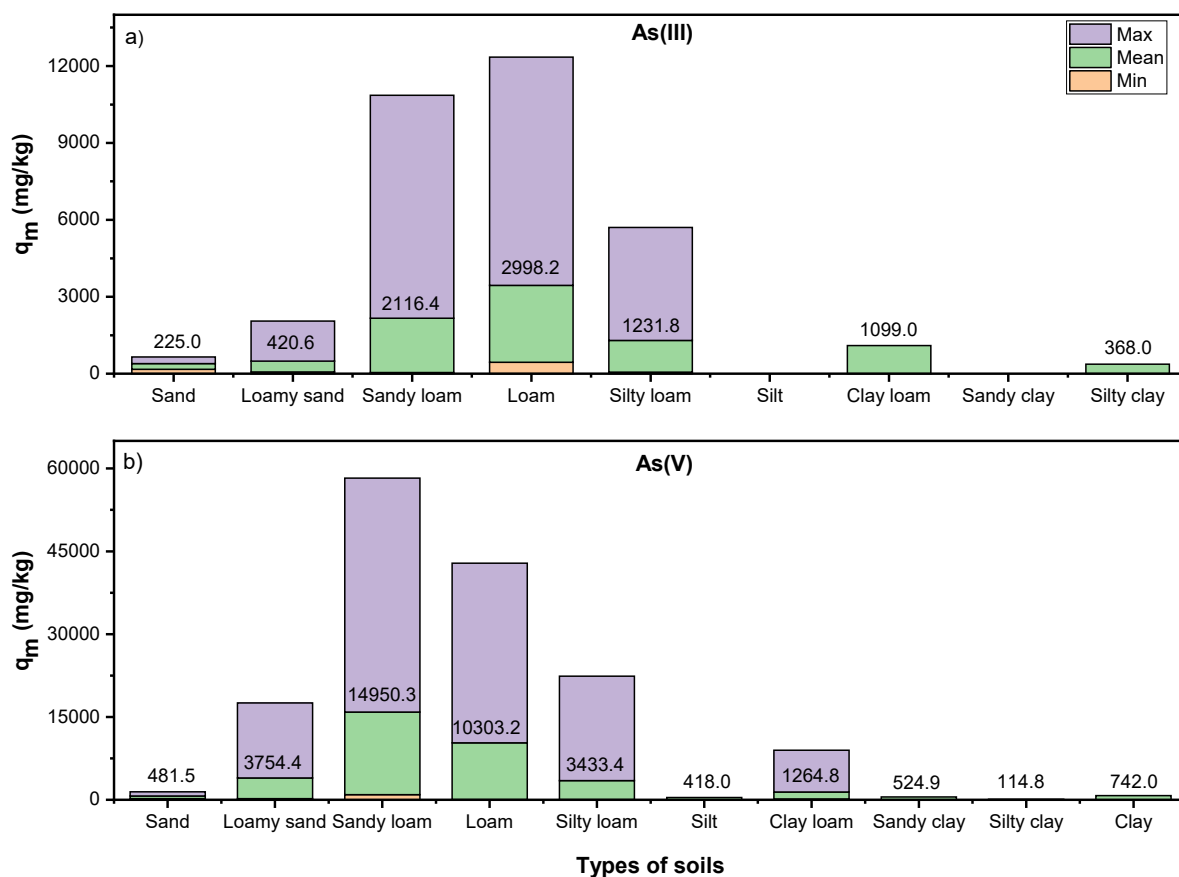
450 where C_e is the equilibrium concentration of arsenic in solution (mg/L or mmol/L), q_e is the amount
451 of arsenic sorbed by soil (mg/kg or mmol/kg) at equilibrium, q_m is the maximum adsorption capacity
452 (mg/kg or mmol/kg), K_L is the Langmuir isotherm constant (L/mg or L/mmol).

453 The linear form of the Langmuir isotherm is described as:

$$454 \quad \frac{C_e}{q_e} = \frac{1}{K_L q_m} + \frac{1}{q_m} C_e \quad (2)$$

455 The values of Langmuir parameters q_m and K_L are calculated from the slope and intercept of the
456 linear plot C_e/q_e versus C_e (Matouq et al., 2015). Based on the data from previous studies, **Fig. 6a** and
457 **6b** illustrates the maximum Langmuir adsorption capacity (q_m) values of As(III) and As(V) on
458 different soils. The selected soils were classified by the USDA soil classification system (García-
459 Gaines and Frankenstein, 2015). The average values of q_m for As(III) ranged from 225 mg/kg on sand

460 soil to 2998.2 mg/kg on loam soil (Fig. 6a), while the results for As(V) varied between 114.8 mg/kg
 461 on silty clay soil and 14950.3 mg/kg on sandy loam soil (Fig. 6b). The highest values of q_m for As(III)
 462 and As(V) were found on loam soil (8901 mg/kg) and sandy loam soil (42400 mg/kg), respectively.
 463 The results show that the maximum soil adsorption capacities were significantly higher for As(V)
 464 than for As(III).



465
 466 **Fig. 6.** The minimum, mean and maximum values of the Langmuir adsorption capacity (q_m) of As(III)
 467 and As(V) adsorption on different soils. Data from Arco-Lázaro et al. (2016), Dias et al (2009), Fan
 468 et al. (2020), Gedik et al. (2016), Huang et al. (2013), Jiang et al. (2005a), Kumar et al. (2016), Luo
 469 et al. (2019), Zhang and Selim (2005).

470
 471 Among different isotherm models, the Langmuir isotherm model exhibited better fit to metal and
 472 metalloid adsorption data than the Freundlich isotherm (Jiang et al., 2005a; Matouq et al., 2015).
 473 According to Gedik et al. (2016), the Langmuir isotherm model was a better fit than using the
 474 Freundlich isotherm model based on statistical correlation with soil properties governing adsorption
 475 for the entire range of As(V) concentrations for different soils. Both Langmuir and Freundlich

476 isotherm models showed very good fit of As(III) and As(V) adsorbed on soil with r^2 values > 0.80
 477 (Dousova et al., 2012; Goldberg and Suarez, 2013; Ma et al., 2015; Wang et al., 2018). Gedik et al.
 478 (2016), Jiang et al. (2005b) and Luo et al. (2019) stated that the Langmuir isotherm model provided
 479 the best fit for all As(V) concentrations based on statistical correlation with soil properties governing
 480 adsorption such as pH, Eh, organic matter, As concentration, and Fe, Al and clay content. The
 481 Langmuir equation (1) is widely known as the Langmuir one-surface equation with hypothesis that
 482 the binding energy for a particular metal or metalloid is the same at all adsorption sites on soils
 483 surfaces (Jiang et al., 2005a). However, in some cases, the plots using the Langmuir one-surface
 484 equation for adsorption data were divided into two straight line portions with different gradients,
 485 indicating that two different types of adsorption sites were available.

486 In order to cope with hypothesis of two different types of adsorption sites, the Langmuir two-
 487 surface equation was developed to plot the adsorption data for both relatively high- and low-energy
 488 surface adsorption sites (Jiang et al., 2005a) as follows:

$$489 \quad q_e = \frac{K_{L1}q_{m1}C_e}{1+K_{L1}C_e} + \frac{K_{L2}q_{m2}C_e}{1+K_{L2}C_e} \quad (3)$$

490 where q_{m1} and K_{L1} represent the adsorption maximum and adsorption equilibrium constant for the
 491 low-energy surface, and q_{m2} and K_{L2} are the adsorption maximum and adsorption equilibrium constant
 492 for the high-energy surface. The total adsorption maximum capacity (q_m) is written as (Jiang et al.,
 493 2005a):

$$494 \quad q_m = q_{m1} + q_{m2} \quad (4)$$

495 The Langmuir maximum sorption capacity and the isotherm constants from the experimental data
 496 vary with the controlling factors. For instance, the variation of the maximum As(V) sorption capacity
 497 of low and high energy surfaces calculated by using a two-surface Langmuir equation in 16 Chinese
 498 soils was 83% and 68%, respectively (Jiang et al., 2015b). Similarly, due to the effect of 0.5 mmol/L
 499 Fe(OH)₃ colloids, the maximum percentage adsorption of As(V) and As(III) was 95% and 64% on
 500 soil from Beijing and 53% and 36% on soil from Jilin, China, respectively while the percentages
 501 reached 98% and 76% for As(V) and As(III) on soil from Hainan, China when Fe(OH)₃ concentration

502 was lower than 0.01 mmol/L (Feng et al., 2013). The results of Feng et al. (2013) also indicated that
 503 As adsorption on three soils in China was favored at high temperature. The adsorption capacities (q_m)
 504 determined from the Langmuir model increased from 13.22 mg/kg to 16.37 mg/kg, 9.96 mg/kg to
 505 19.46 mg/kg and 23.27 mg/kg to 27.08 mg/kg for soils from Beijing, Jilin and Hainan, China when
 506 the temperature was increased from 283 K to 323 K. Kundu and Gupta (2006) showed similar results
 507 for both As(V) and As(III) adsorption capacities onto iron oxide-coated cement under three
 508 temperatures (288 K, 298 K and 308 K). In addition, adsorption maximum of As(V) calculated by
 509 the Langmuir equation increased with reaction time from 92.2 mg/kg, 263.0 mg/kg and 169.2 mg/kg
 510 in the first 6 h to 418.2 mg/kg, 742.0 mg/kg and 554.9 mg/kg at 504 h for Olivier loam, Sharkey clay
 511 and Windsor sand, respectively (Zhang and Selim, 2005). For As(III), the maximum adsorption on
 512 irrigated soil was 368 mg/kg (Huang et al., 2013).

513 Generally, the maximum Langmuir adsorption capacities of As(III) were higher than those of
 514 As(V), e.g. 1040 $\mu\text{g/g}$ vs 520 $\mu\text{g/g}$ by natural siderite (Guo et al., 2007), 180.3 mg/g vs 172.1 mg/g
 515 by iron oxide-graphene (Mishra and Ramaprabhu, 2012), and 7.7 mmol/kg vs 5.0 mmol/kg by natural
 516 soil (Dousova et al., 2012) for As(III) and As(V), respectively. However, Wang et al. (2018) reported
 517 a higher maximum adsorption capacity of As(V) at 6.949 $\mu\text{mol/g}$ than for As(III) at 4.044 $\mu\text{mol/g}$ by
 518 lake and river sediments in China.

519 During the two types of surface modelling, Jiang et al. (2005b) established the relationship
 520 between the adsorption maximum, two-surface adsorption sites, and soils properties by using
 521 stepwise multiple linear regression. The best regression models describing the relationship between
 522 the adsorption maximum on the low-energy surface (q_{m1}), high-energy surface (q_{m2}) and individual
 523 soil properties are described in **Table 2**.

524
 525 **Table 2.** The stepwise regressions for As(V) adsorption maximum capacity on low-energy surface
 526 (q_{m1}) and high-energy surface (q_{m2}) (Jiang et al., 2005b)

Model	Multiple linear equation	r^2	Standard error of the estimate
-------	--------------------------	-------	-----------------------------------

The stepwise regression for q_{m1}			
1	$q_{m1} = 0.050[\text{Fe}_{\text{CD}}] - 73.757$	0.834	48.41
2	$q_{m1} = 0.040[\text{Fe}_{\text{CD}}] + 3.847[\text{Clay}] - 135.527$	0.889	41.18
3	$q_{m1} = 0.034[\text{Fe}_{\text{CD}}] + 6.317[\text{Clay}] - 13.419[\text{SOM}] - 145.404$	0.922	35.87
4	$q_{m1} = 0.032[\text{Fe}_{\text{CD}}] + 6.758[\text{Clay}] - 10.228[\text{SOM}] - 0.096[\text{DOC}] - 116.190$	0.938	33.45
The stepwise regression for q_{m2}			
1	$q_{m2} = 0.018[\text{Fe}_{\text{CD}}] - 55.141$	0.682	26.69
2	$q_{m2} = 0.018[\text{Fe}_{\text{CD}}] - 0.093[\text{DOC}] - 13.117$	0.810	21.41
3	$q_{m2} = 0.019[\text{Fe}_{\text{CD}}] - 0.095[\text{DOC}] - 3.609[\text{As}] + 9.549$	0.876	17.92

527 Fe_{CD} : citrate-dithionite extractable Fe; DOC: dissolved organic carbon; As: total As.

528

529 The contents of Fe_{CD} , clay, SOM and DOC contributed to nearly 94% of the variability in As(V)
530 adsorption on the low-energy surface while Fe_{CD} , DOC and total As concentrations in soils accounted
531 for nearly 88% of the variability in As(V) adsorption on the high-energy surface. **Table 2** shows that
532 the contents of Fe_{CD} and clay enhance the adsorption capacities of As(V) while SOM, DOC and total
533 As concentration reduce the adsorption capacities in both high- and low-energy surface sites. Thus,
534 the Langmuir isotherm model can provide a good fit of As adsorption in both high-energy and low-
535 energy adsorption sites.

536

537 **4.2. The Freundlich isotherm model**

538 The empirical equation of the Freundlich adsorption isotherm is most often used in the description
539 of adsorption (Aksentijević et al., 2012; Wang et al., 2018):

$$540 \quad q_e = K_F \times C_e^{1/n} \quad (5)$$

541 where K_F is the Freundlich constant or capacity factor ($\text{mg}^{1-1/n} \text{L}^{1/n}/\text{kg}$), while $1/n$ is the Freundlich
542 exponent.

543 The Freundlich isotherm model can be transformed to a linear form as:

$$544 \quad \ln q_e = \ln K_F + \frac{1}{n} \ln C_e \quad (6)$$

545 These isothermal constants are very important for understanding the mechanism of adsorption
546 (Aksentijević et al., 2012). The empirical constants K_F and $1/n$ represent the curvature and steepness

547 of the isotherm, indicating adsorption capacity and intensity of the adsorption process. The values of
548 $1/n$ ranged from 0 to 1 indicating the favorable adsorption of As onto adsorbents (Arco-Lázaro et al.,
549 2016; Guo et al., 2007). **Fig. 6b** exhibits the Freundlich constant or adsorption capacity (K_F) of As(III)
550 and As(V) adsorbed on soil. It can be seen that the average adsorption capacity for As(V) adsorbed
551 on soils was 359.7 mL/g ($n = 11$), which is over ten times that of As(III) at 33.1 mL/g ($n = 10$).

552 Similar to the Langmuir adsorption capacity (q_m), the Freundlich adsorption constant K_F
553 increased from 1.94 to 4.71 (mg/kg) (L/mg)^{1/n}, 0.58 to 0.77 (mg/kg) (L/mg)^{1/n} and 3.59 to 5.38
554 (mg/kg) (L/mg)^{1/n} for soils from Beijing, Jilin and Hainan, China with the increase in temperature
555 from 283 K to 323 K (Feng et al., 2013). The linear adsorption constant (K_d) for As(V) adsorption on
556 saline-alkali soils varied between 86.0 mL/g and 157.1 mL/g (Luo et al., 2019). The study of Kumar
557 pointed out that the Freundlich isotherm model exhibited better results for As(V) adsorption on soils
558 than As(III) due to several low r^2 values of regressions for As(III) at 0.03, 0.12 and 0.34, respectively.

559 Furthermore, Kundu and Gupta (2006) showed that the Freundlich isotherm model was a better fit
560 for both As(V) and As(III) sorption in linear and nonlinear systems at different temperatures (288, 298
561 and 308 K) compared to the Langmuir, Dubinin-Radushkevich (D-R) and Toth and Temkin isotherm
562 equations. The adsorption of As(V) was highly nonlinear with the Freundlich isotherm on Olivier loam,
563 Sharkey clay and Windsor sand soils (Zhang and Selim, 2005) and on carbonate-rich soils (Yocubal
564 and Akyol, 2008). Similarly, the Freundlich isotherm equation provided a better fit than the Langmuir,
565 Temkin and Dubinin-Radushkevich isotherm models (Huang et al., 2013), for As(III) adsorption
566 process in contaminated agricultural soil from an irrigated area, China. In another study, Guo et al.,
567 (2007) showed that the Freundlich isotherm exhibited a better fit than the Langmuir isotherm to the
568 experimental data for the smaller grain size of the natural siderite (0.10-0.25 mm), whilst the two models
569 were comparable for the grain size range of 0.25-0.5 mm. The study of Arco-Lázaro et al. (2016) also
570 showed the better fitting results of As(V) adsorption by soils using the Freundlich isotherm equation
571 than the Langmuir isotherm equation. Therefore, it can be concluded that the Freundlich isotherm model
572 can well describe the adsorption of both As(III) and As(V) on soil in terms of nonlinear systems.

573

574 **4.3. Modified Langmuir-Freundlich (MLF) isotherm model**

575 Based on both Langmuir and Freundlich types for adsorption behaviour of As, a general form of
576 the Langmuir-Freundlich isotherm equation for As(V) adsorption was proposed (Jeppu and Clement,
577 2012):

$$578 \quad q_e = \frac{Q_m(K_a C_e)^{1/n}}{(K_a C_e)^{1/n} + 1} \quad (7)$$

579 where Q_m is the maximum adsorption capacity of the system (mg/g), K_a is the affinity constant for
580 adsorption (L/mg), $1/n$ is the index of heterogeneity which varies from 0 to 1.

581 Mathematically, when $1/n$ is set to 1, Eq. (7) is simplified to:

$$582 \quad q_e = Q_m \frac{K_a C_e}{1 + K_a C_e} \quad (8)$$

583 Eq. (8) is identical to the Langmuir isotherm with a pH-dependent sorption capacity value. When C_e
584 or K_a reaches a low value, Eq. (7) will be reduced to a Freundlich type expression.

585 Using the experimental data of As(V) adsorption, Jeppu and Clement (2012) plotted the
586 relationship between affinity constant (K_a) against pH for goethite-coated sand (Eq. 9) and pure
587 goethite (Eq. 10):

$$588 \quad \log K_a = -0.73 \text{ pH} + 5.8 \quad (9)$$

$$589 \quad \log K_a = -0.95 \text{ pH} + 7.35 \quad (10)$$

590 Eq. (9) showed that the value of $\log K_a$ decreased linearly with increasing pH, which was
591 explained by the increase in positively charged surface species ($>\text{FeOOH}_2^+$) expressing higher
592 affinity for adsorbing the negatively charged As(V) ions (Jeppu and Clement, 2012). As a result, the
593 model parameters (Q_m , $1/n$) estimated for MLF isotherm were 0.097 and 0.412 for goethite-coated
594 sand and 10.5 and 0.333 for pure goethite, respectively. Subsequently, the MLF model was
595 successfully used to predict the experimental pH edges observed at four different initial As(V)
596 concentrations (7.5, 3.8, 1.9 and 0.75 mg/L) for As(V) adsorption on pure goethite (Jeppu and
597 Clement, 2012).

598 In summary, the Langmuir model assumes the adsorption occurring on a homogeneous adsorbent
599 surface, while the Freundlich model describes multi-layers of adsorption process (Ma et al., 2015).
600 Neither Langmuir nor Freundlich isotherm explains the mechanism of adsorption, whilst Temkin and
601 D-R isotherms can (Kumar et al., 2016). The authors pointed out that the Temkin factors including
602 adsorption potentials (A_T) and constant for energy of adsorption (B) can illustrate the
603 thermodynamics of adsorbate-adsorbent interactions, specifically a uniform distribution of binding
604 energies via the function of temperature. The D-R isotherm uses a Gaussian energy distribution on a
605 heterogeneous surface, which considers a function of C_e and temperature to express the adsorption
606 mechanism. It is assumed that the adsorption experiments of As(III) and As(V) on soils have been
607 conducted in different conditions leading to the large variation of maximum adsorption capacity (q_m)
608 and adsorption capacity factor (K_F). However, both the Langmuir and Freundlich models have been
609 widely applied to evaluate the maximum adsorption capacity (q_m or K_F) of adsorbents regardless of
610 controlling parameters.

611

612 **5. Future perspectives and implications for managing As-contaminated soil**

613 Based on the extensive literature review, this study has identified that the most highly As-
614 contaminated soil was found in Chihuahua region, Mexico with 116000 mg/kg of As, whilst the
615 highest Langmuir adsorption capacity of soils was 42400 mg/kg for Dunellen sandy loam from New
616 Jersey, USA (Dias et al., 2009). In addition, the most important control factors of As adsorption on
617 soil are soil pH, clay mineral and texture. Therefore, in order to manage soil contamination by As,
618 there are a few lessons that can be learnt. First, the sources of As contamination should be identified
619 as soon as feasible, in order to prevent further discharge (e.g. from mining sites) and movement of
620 contamination beyond the affected areas. Secondly, As contamination hotspots and chemical
621 speciation (As(III), As(V)) should be determined through well-designed field sampling and chemical
622 analyses with good quality control, to overcome the challenges of heterogeneity and uncertainty in
623 soil contamination investigations (Zhou et al., 2014). Thirdly, the fundamental properties of soil

624 should be determined including pH, clay mineral and texture. Such detailed information will aid the
625 confirmation of dominating As species and sorption mechanism, such as As(V) in acidic and
626 oxidizing soil by chemisorption and As(III) in high pH and reducing soil by physisorption. Therefore,
627 the decontamination of As-contaminated soils can be achieved to a high standard using effective and
628 environmentally friendly technologies such as magnetic biochar (Wan et al., 2020) and electrokinetic
629 technology incorporating reactive filter media (Ghobadi et al., 2021) which can simultaneously
630 remove multiple heavy metals from soil.

631

632 **6. Conclusions**

633 The extent of As contamination in soils globally has been systematically reviewed, with the
634 highest concentration of As contamination at 116000 mg/kg being reported in Mexico caused by
635 mining activities. Highly As contaminated mining soils were also reported in several European
636 countries and Iran. Soil pH, clay mineral and texture were the most important controlling factors
637 positively affecting the adsorption of As(III) and As(V) on soils. Other soil properties including SOM,
638 anions and bacteria had small and negative influences on As adsorption. The maximum adsorption
639 capacity was 230 mg/kg of As(III) for tropical soil at pH 7, and 1875 mg/kg of As(V) for paddy soil
640 at pH 3. Both Langmuir and Freundlich isotherms well described As adsorption in soils, with the
641 values of q_m being 45-8901 mg/kg for As(III) and 22-42400 mg/kg for As(V). Future studies should
642 be focused on comprehensive statistical analysis of large datasets of As contamination levels in
643 relation to a full range of soil properties under contrasting hydrogeological conditions, in order to
644 unravel the most critical fundamental control of As contamination in the soil environment. Such
645 detailed assessment will enable the remediation of As-contaminated soils to be more targeted and
646 effective.

647

648 **Acknowledgements**

649 We acknowledge the support from the 111 Project (D18012).

650 **References**

- 651 Abedi, T., Mojiri, A., Arsenic uptake and accumulation mechanisms in rice species. *Plants* 9(2), 129.
- 652 Aksentijević, S., Kiurski, J., Vasić, M. V., 2012. Arsenic distribution in water/sediment system of
653 Sevojno. *Environ. Monit. Assess.* 184, 335-341.
- 654 Akter, K. F., Owens, G., Davey, D. E., Naidu, R., 2005. Arsenic speciation and toxicity in biological
655 systems. *Rev. Environ. Contam. Toxicol.* 184, 97-149.
- 656 Alloway, B. J., 2013. Sources of heavy metals and metalloids in soils. In *Heavy Metals in Soils* (pp.
657 11-50), Springer.
- 658 Álvarez-Benedí, J., Bolado, S., Cancillo, I., Calvo, C., Garcia-Sinovas, D., 2005. Adsorption–
659 desorption of arsenate in three Spanish soils. *Vadose Zone J.* 4, 282-290.
- 660 Antelo, J., Arce, F., Fiol, S., 2015. Arsenate and phosphate adsorption on ferrihydrite nanoparticles.
661 Synergetic interaction with calcium ions. *Chem. Geol.* 410, 53-62.
- 662 Antelo, J., Avena, M., Fiol, S., López, R., Arce, F., 2005. Effects of pH and ionic strength on the
663 adsorption of phosphate and arsenate at the goethite–water interface. *J. Colloid Interface Sci.* 285,
664 476-486.
- 665 Arco-Lázaro, E., Agudo, I., Clemente, R., Bernal, M. P., 2016. Arsenic (V) adsorption-desorption in
666 agricultural and mine soils: effects of organic matter addition and phosphate competition.
667 *Environ. Pollut.* 216, 71-79.
- 668 Bhattacharya, S., Sharma, P., Mitra, S., Mallick, I., Ghosh, A., 2021. Arsenic Uptake and
669 Bioaccumulation in Plants: A Review on Remediation and Socio-Economic Perspective in
670 Southeast Asia. *Environ. Nanotechnol. Monit. Manag.* 100430.
- 671 Basu, A., Saha, D., Saha, R., Ghosh, T., Saha, B., 2014. A review on sources, toxicity and remediation
672 technologies for removing arsenic from drinking water. *Res. Chem. Intermed.* 40, 447-485.
- 673 Baviskar, S., Choudhury, R., Mahanta, C., 2015. Dissolved and solid-phase arsenic fate in an arsenic-
674 enriched aquifer in the river Brahmaputra alluvial plain. *Environ. Monit. Assess.* 187, 93.
- 675 Bhuiyan, M. A. H., Karmaker, S. C., Bodrud-Doza, M., Rakib, M. A., Saha, B. B., 2021. Enrichment,
676 sources and ecological risk mapping of heavy metals in agricultural soils of dhaka district
677 employing SOM, PMF and GIS methods. *Chemosphere* 263, 128339.
- 678 Bundschuh, J., Armienta, M.A., Morales-Simfors, N., Alam, M.A., López, D.L., Quezada, V.D.,
679 Dietrich, S., Schneider, J., Tapia, J., Sracek, O., Castillo, E., Parra, L.M.M., et al., 2020. Arsenic
680 in Latin America: New findings on source, mobilization and mobility in human environments in
681 20 countries based on decadal research 2010-2020. *Crit. Rev. Environ. Sci. Technol.*
682 <https://doi.org/10.1080/10643389.2020.1770527>.

683 Cao, X., Gao, X., Zeng, X., Ma, Y., Gao, Y., Baeyens, W., et al., 2021. Seeking for an optimal strategy
684 to avoid arsenic and cadmium over-accumulation in crops: Soil management vs cultivar selection
685 in a case study with maize. *Chemosphere* 272, 129891.

686 Campbell, K. M., Nordstrom, D. K., 2014. Arsenic speciation and sorption in natural environments.
687 *Rev. Mineral. Geochem* 79, 185-216.

688 Caporale, A., Pigna, M., Azam, S., Sommella, A., Rao, M., Violante, A., 2013. Effect of competing
689 ligands on the sorption/desorption of arsenite on/from Mg-Fe layered double hydroxides (Mg-
690 Fe-LDH). *Chem. Eng. J.* 225, 704-709.

691 Carrillo-Chavez, A., Salas-Megchun, E., Levresse, G., Munoz-Torres, C., Perez-Arvizu, O., Gerke,
692 T., 2014. Geochemistry and mineralogy of mine-waste material from a “skarn-type” deposit in
693 central Mexico: Modeling geochemical controls of metals in the surface environment. *J.*
694 *Geochem. Explor.* 144, 28-36.

695 Casado, M., Anawar, H., Garcia-Sanchez, A., Santa Regina, I., 2007. Antimony and arsenic uptake
696 by plants in an abandoned mining area. *Commun. Soil Sci. Plant Anal.* 38(9-10), 1255-1275.

697 de Brouwere, K., Smolders, E., Merckx, R., 2004. Soil properties affecting solid-liquid distribution
698 of As (V) in soils. *Eur. J. Soil Sci.* 55(1), 165-173.

699 de Figueiredo, B.R., Borba, R.P., Angélica, R.S., 2007. Arsenic occurrence in Brazil and human
700 exposure. *Environ. Geochem. Health* 29, 109-118.

701 Deng, Y., Li, Y., Li, X., Sun, Y., Ma, J., Lei, M., Weng, L., 2018. Influence of calcium and phosphate
702 on pH dependency of arsenite and arsenate adsorption to goethite. *Chemosphere* 199, 617-624.

703 Dias, F. F., Allen, H. E., Guimarães, J. R., Taddei, M. H. T., Nascimento, M. R., Guilherme, L. R.
704 G., 2009. Environmental behavior of arsenic (III) and (V) in soils. *J. Environ. Monit.* 11, 1412-
705 1420.

706 Dong, G., Han, R., Pan, Y., Zhang, C., Liu, Y., Wang, H., et al., 2021. Role of MnO₂ in controlling
707 iron and arsenic mobilization from illuminated flooded arsenic-enriched soils. *J. Hazard. Mater.*
708 401, 123362.

709 Dousova, B., Buzek, F., Rothwell, J., Krejcova, S., Lhotka, M., 2012. Adsorption behavior of arsenic
710 relating to different natural solids: Soils, stream sediments and peats. *Sci. Total Environ.* 433,
711 456-461.

712 Fan, Y., Zheng, C., Liu, H., He, C., Shen, Z., Zhang, T. C., 2020. Effect of pH on the adsorption of
713 arsenic(V) and antimony(V) by the black soil in three systems: Performance and mechanism.
714 *Ecotoxicol. Environ. Saf.* 191, 110145.

715 Farrell, J., 2017. Tridentate arsenate complexation with ferric hydroxide and its effect on the kinetics
716 of arsenate adsorption and desorption. *Chemosphere* 184, 1209-1214.

717 Fleck, A. T., Mattusch, J., Schenk, M. K., 2013. Silicon decreases the arsenic level in rice grain by
718 limiting arsenite transport. *J. Plant Nutr. Soil Sci.* 176(5), 785-794.

719 Fendorf, S., Nico, P. S., Kocar, B. D., Masue, Y. Tufano, K. J., 2010. Arsenic chemistry in soils and
720 sediments. *Developments in Soil Science* 34, Elsevier 2010, 357-378.

721 Feng, Q., Zhang, Z., Chen, Y., Liu, L., Zhang, Z., Chen, C., 2013. Adsorption and desorption
722 characteristics of arsenic on soils: kinetics, equilibrium, and effect of Fe(OH)₃ colloid, H₂SiO₃
723 colloid and phosphate. *Procedia Environ. Sci.* 18, 26-36.

724 Foo, K. Y., Hameed, B. H., 2010. Insights into the modeling of adsorption isotherm systems. *Chem.*
725 *Eng. J.* 156(1), 2-10.

726 Foroutan, R., Mohammadi, R., Adeleye, A. S., Farjadfard, S., Esvandi, Z., Arfaeinia, H., Sorial, G.
727 A., Ramavandi, B., Sahebi, S., 2019. Efficient arsenic (V) removal from contaminated water
728 using natural clay and clay composite adsorbents. *Environ. Sci. Pollut. Res.* 26(29), 29748-29762.

729 García-Gaines, R. A., Frankenstein, S., 2015. USCS and the USDA soil classification system:
730 Development of a mapping scheme.

731 Gedik, K., Kongchum, M., Boran, M., Delaune, R. D., 2016. Adsorption and desorption of arsenate
732 in Louisiana rice soils. *Arch. Agron. Soil Sci.* 62(6), 856-864.

733 Gemici, Ü., Tarcan, G., 2007. Assessment of the pollutants in farming soils and waters around
734 untreated abandoned Türkönü mercury mine (Turkey). *B. Environ. Contam Tox.* 79, 20-24.

735 Gerdelidani, A. F., Towfighi, H., Shahbazi, K., Lamb, D. T., Choppala, G., Abbasi, S., et al., 2021.
736 Arsenic geochemistry and mineralogy as a function of particle-size in naturally arsenic-enriched
737 soils. *J. Hazard. Mater.* 403, 123931.

738 Ghobadi, R., Altaee, A., Zhou, J.L., Karbassiyazdi, E., Ganbat, N., 2021. Effective remediation of
739 heavy metals in contaminated soil by electrokinetic technology incorporating reactive filter
740 media. *Sci. Total Environ.* 794, 148668.

741 Ghosal, P. S., Gupta, A. K., 2017. Development of a generalized adsorption isotherm model at solid-
742 liquid interface: A novel approach. *J. Mol. Liq.* 240, 21-24.

743 Gitari, M. W., Mudzielwana, R., 2018. Mineralogical and Chemical Characteristics of Raw and
744 Modified Clays and Their Application in Arsenic and Fluoride Removal. *Current Topics in the*
745 *Utilization of Clay in Industrial and Medical Applications*, 45.

746 Goh, K. H., Lim, T. T., 2004. Geochemistry of inorganic arsenic and selenium in a tropical soil: effect
747 of reaction time, pH, and competitive anions on arsenic and selenium adsorption. *Chemosphere*
748 55, 849-859.

749 Goldberg, S., 2002. Competitive adsorption of arsenate and arsenite on oxides and clay minerals.
750 *Soil Sci. Soc. Am.* 66(2), 413-421.

751 Goldberg, S., Lesch, S. M., Suarez, D. L., Basta, N. T., 2005. Predicting Arsenate Adsorption by Soils
752 using Soil Chemical Parameters in the Constant Capacitance Model. *Soil Sci. Soc. Am.* 69(5),
753 1389-1398.

754 Goldberg, S., Suarez, D. L., 2013. Arsenate adsorption by unsaturated alluvial sediments. *Soil Sci.*
755 *Soc. Am.* 77(3), 782-791.

756 Grafe, M., Eick, M. Grossl, P., 2001. Adsorption of arsenate (V) and arsenite (III) on goethite in the
757 presence and absence of dissolved organic carbon. *Soil Sci. Soc. Am.* 65, 1680-1687.

758 Guo, H., Stüben, D., Berner, Z., 2007. Adsorption of arsenic (III) and arsenic (V) from groundwater
759 using natural siderite as the adsorbent. *J. Colloid Interface Sci.* 315(1), 47-53.

760 Gustafsson, J. P., 2006. Arsenate adsorption to soils: Modelling the competition from humic
761 substances. *Geoderma* 136(1-2), 320-330.

762 Hayat, K., Menhas, S., Bundschuh, J., Chaudhary, H. J., 2017. Microbial biotechnology as an
763 emerging industrial wastewater treatment process for arsenic mitigation: A critical review. *J.*
764 *Clean. Prod.* 151, 427-438.

765 Huang, G., Chen, Z., Wang, J., Sun, J., Liu, J., Zhang, Y., 2013. Adsorption of arsenite onto a soil
766 irrigated by sewage. *J. Geochem. Explor.* 132, 164-172.

767 Huang, J.H., 2018. Characterising microbial reduction of arsenate sorbed to ferrihydrite and its
768 concurrence with iron reduction. *Chemosphere* 194, 49-56.

769 Huang, R.Q., Gao, S.F., Wang, W.L., Staunton, S., Wang, G., 2006. Soil arsenic availability and the
770 transfer of soil arsenic to crops in suburban areas in Fujian Province, southeast China. *Sci. Total*
771 *Environ.* 368(2-3), 531-541.

772 Huling, J.R., Huling, S.G., Ludwig, R., 2017. Enhanced adsorption of arsenic through the oxidative
773 treatment of reduced aquifer solids. *Water Res.* 123, 183-191.

774 Jana, U., Chassany, V., Bertrand, G., Castrec-Rouelle, M., Aubry, E., Boudsocq, S. Laffray, D.,
775 Repellin, A., 2012. Analysis of arsenic and antimony distribution within plants growing at an old
776 mine site in Ouche (Cantal, France) and identification of species suitable for site revegetation. *J.*
777 *Environ. Manage.* 110, 188-193.

778 Jeppu, G. P., Clement, T. P., 2012. A modified Langmuir-Freundlich isotherm model for simulating
779 pH-dependent adsorption effects. *J. Contam. Hydrol.* 129-130, 46-53.

780 Jia, X., Cao, Y., O'Connor, D., Zhu, J., Tsang, D. C., Zou, B., et al., 2021. Mapping soil pollution by
781 using drone image recognition and machine learning at an arsenic-contaminated agricultural
782 field. *Environ. Pollut.* 270, 116281.

783 Jiang, J., Dai, Z., Sun, R., Zhao, Z., Dong, Y., Hong, Z., Xu, R., 2017. Evaluation of ferrollysis in
784 arsenate adsorption on the paddy soil derived from an Oxisol. *Chemosphere* 179, 232-241.

- 785 Jiang, W., Zhang, S., Shan, X.-q., Feng, M., Zhu, Y.-G., McLaren, R. G., 2005a. Adsorption of
786 arsenate on soils. Part 1: Laboratory batch experiments using 16 Chinese soils with different
787 physiochemical properties. *Environ. Pollut.* 138(2), 278-284.
- 788 Jiang, W., Zhang, S., Shan, X.-q., Feng, M., Zhu, Y.-G., McLaren, R. G., 2005b. Adsorption of
789 arsenate on soils. Part 2: Modeling the relationship between adsorption capacity and soil
790 physiochemical properties using 16 Chinese soils. *Environ. Pollut.* 138(2), 285-289.
- 791 Jlassi, K., Krupa, I., Chehimi, M. M., 2017. Overview: clay preparation, properties, modification. In
792 *Clay-polymer nanocomposites* (pp. 1-28): Elsevier.
- 793 Johnston, S. G., Bennett, W. W., Doriean, N., Hockmann, K., Karimian, N., Burton, E. D., 2020.
794 Antimony and arsenic speciation, redox-cycling and contrasting mobility in a mining-impacted
795 river system. *Sci. Total Environ.* 710, 136354.
- 796 Kebonye, N. M., John, K., Chakraborty, S., Agyeman, P. C., Ahado, S. K., Eze, P. N., et al., 2021.
797 Comparison of multivariate methods for arsenic estimation and mapping in floodplain soil via
798 portable X-ray fluorescence spectroscopy. *Geoderma* 384, 114792.
- 799 Kumar, R., Kumar, R., Mittal, S., Arora, M., Babu, J. N., 2016. Role of soil physicochemical
800 characteristics on the present state of arsenic and its adsorption in alluvial soils of two agri-
801 intensive region of Bathinda, Punjab, India. *J. Soils Sediments* 16, 605-620.
- 802 Kundu, S. Gupta, A., 2006. Arsenic adsorption onto iron oxide-coated cement (IOCC): regression
803 analysis of equilibrium data with several isotherm models and their optimization. *Chem. Eng. J.*
804 122, 93-106.
- 805 Lebrun, M., Van Poucke, R., Miard, F., Scippa, G. S., Bourgerie, S., Morabito, D., et al., 2021. Effects
806 of carbon-based materials and redmuds on metal (loid) immobilization and growth of *Salix*
807 *dasyclados* Wimm. on a former mine technosol contaminated by arsenic and lead. *Land Degrad.*
808 *Dev.* 32(1), 467-481.
- 809 Lombi, E., Holm, P. E., 2010. Metalloids, soil chemistry and the environment. In *MIPs and Their*
810 *Role in the Exchange of Metalloids* (pp. 33-44): Springer.
- 811 Luo, T., Sun, J., Liu, Y., Cui, L., Fu, Q., 2019. Adsorption and transport behavior of arsenate on
812 saline-alkali soils of tidal flat of Yellow Sea, Eastern China. *Env. Pollut. Bioavail.* 31(1), 166-
813 173.
- 814 Macht, F., Eusterhues, K., Pronk, G. J., Totsche, K. U., 2011. Specific surface area of clay minerals:
815 Comparison between atomic force microscopy measurements and bulk-gas (N₂) and-liquid
816 (EGME) adsorption methods. *Appl. Clay Sci.* 53(1), 20-26.
- 817 Maji, S. K., Pal, A., Pal, T., Adak, A., 2007. Modeling and fixed bed column adsorption of As(III) on
818 laterite soil. *Sep. Purif. Technol.* 56(3), 284-290.

819 Martin, M., Violante, A., Ajmone-Marsan, F., Barberis, E., 2014. Surface interactions of arsenite and
820 arsenate on soil colloids. *Soil Sci. Soc. Am.* 78(1), 157-170.

821 Masri, S., LeBrón, A. M., Logue, M. D., Valencia, E., Ruiz, A., Reyes, A., et al., 2021. Risk
822 assessment of soil heavy metal contamination at the census tract level in the city of Santa Ana,
823 CA: implications for health and environmental justice. *Environ. Sci. Process Impacts* DOI:
824 10.1039/d1em00007a

825 Matouq, M., Jildeh, N., Qtaishat, M., Hindiyeh, M., Al Syouf, M. Q., 2015. The adsorption kinetics
826 and modeling for heavy metals removal from wastewater by Moringa pods. *J. Environ. Chem.*
827 *Eng.* 3(2), 775-784.

828 McCarty, K.M., Hanh, H.T., Kim, K.W., 2011. Arsenic geochemistry and human health in South East
829 Asia. *Rev Environ Health* 26(1), 71-78.

830 Mishra, A. K., Ramaprabhu, S., 2012. Ultrahigh arsenic sorption using iron oxide-graphene
831 nanocomposite supercapacitor assembly. *J. Appl. Phys.* 112(10), 104315.

832 Mohan, D., Pittman JR, C. U., 2007. Arsenic removal from water/wastewater using adsorbents—a
833 critical review. *J. Hazard. Mater.* 142, 1-53.

834 Mohapatra, D., Mishra, D., Chaudhury, G.R., Das, R.P., 2007. Arsenic adsorption mechanism
835 on clay minerals and its dependence on temperature. *Korean J. Chem. Environ.* 24, 426-430.

836 Mukhopadhyay, R., Manjaiah, K., Datta, S., Yadav, R., Sarkar, B., 2017. Inorganically modified clay
837 minerals: Preparation, characterization, and arsenic adsorption in contaminated water and soil.
838 *Appl. Clay Sci.* 147, 1-10.

839 Neidhardt, H., Kramar, U., Tang, X., Guo, H., Norra, S., 2015. Arsenic accumulation in the roots of
840 *Helianthus annuus* and *Zea mays* by irrigation with arsenic-rich groundwater: Insights from
841 synchrotron X-ray fluorescence imaging. *Geochemistry* 75(2), 261-270.

842 Nguyen, K.T., Nguyen, H.M., Truong, C.K., Ahmed, M.B., Huang, Y., Zhou, J.L. (2019) Chemical
843 and microbiological risk assessment of urban river water quality in Vietnam. *Environ. Geochem.*
844 *Health* 41, 2559-2575.

845 Ong, G.H., Yap, C.K., Maziah, M., Suhaimi, H., Tan, S.G., 2013. An investigation of arsenic
846 contamination in Peninsular Malaysia based on *Centella asiatica* and soil samples. *Environ.*
847 *Monit. Assess.* 185, 3243-3254.

848 Osuna-Martínez, C. C., Armienta, M. A., Bergés-Tiznado, M. E., Páez-Osuna, F., 2020. Arsenic in
849 waters, soils, sediments, and biota from Mexico: An environmental review. *Sci. Total Environ.*
850 142062.

851 Orosun, M. M., 2021. Assessment of arsenic and its associated health risks due to mining activities
852 in parts of North-central Nigeria: Probabilistic approach using Monte Carlo. *J. Hazard. Mater.*
853 412, 125262.

854 Qiu, G., Gao, T., Hong, J., Luo, Y., Liu, L., Tan, W., Liu, F., 2018. Mechanisms of interaction
855 between arsenian pyrite and aqueous arsenite under anoxic and oxic conditions. *Geochim.*
856 *Cosmochim. Acta.* 228, 205-219.

857 Rapant, S., Dietzová, Z., Cicmanová, S., 2006. Environmental and health risk assessment in
858 abandoned mining area, Zlata Idka, Slovakia. *Environ. Geol.* 51(3), 387-397.

859 Reid, M. S., Hoy, K. S., Schofield, J. R., Uppal, J. S., Lin, Y., Lu, X., Peng, H., Le, X. C., 2020.
860 Arsenic speciation analysis: A review with an emphasis on chromatographic separations. *Trends*
861 *Anal. Chem.* 123, 115770.

862 Renkou, X., Yong, W., Tiwari, D., Houyan, W., 2009. Effect of ionic strength on adsorption of As
863 (III) and As (V) on variable charge soils. *J. Environ. Sci.* 21(7), 927-932.

864 Rezaei, H., Mehrabi, B., Khanmirzaee, A., Shahbazi, K., 2021. Arsenic heavy metal mapping in
865 agricultural soils of Alborz province, Iran. *Int. J. Environ. Anal. Chem.* 101(1), 127-139.

866 Selim, H. M., 2012. *Competitive Sorption and Transport of Heavy Metals in Soils and Geological*
867 *Media.* CRC Press.

868 Smedley, P. L., Kinniburgh, D., 2002. A review of the source, behaviour and distribution of arsenic
869 in natural waters. *Appl. Geochem.* 17(5), 517-568.

870 Smith E, Smith J, Smith L, Biswas T, Correll R, Naidu R., 2003. Arsenic in Australian environment:
871 an overview. *J. Environ. Sci. Heal. A.* 38, 223-239.

872 Smith, E., Smith, J., Naidu, R., 2006. Distribution and nature of arsenic along former railway
873 corridors of South Australia. *Sci. Total Environ.* 363, 175-182.

874 Smith, E., Naidu, R., Alston, A. M., 2002. Chemistry of Inorganic Arsenic in Soils: II. Effect of
875 Phosphorus, Sodium, and Calcium on Arsenic Sorption. *J. Environ. Qual.* 31(2), 557.

876 Stollenwerk, K. G., 2003. Geochemical processes controlling transport of arsenic in groundwater: a
877 review of adsorption. In *Arsenic in ground water* (pp. 67-100), Springer.

878 Szopka, K., Gruss, I., Gruszka, D., Karczewska, A., Gediga, K., Gałka, B., et al., 2021. The Effects
879 of Forest Litter and Waterlogging on the Ecotoxicity of Soils Strongly Enriched in Arsenic in a
880 Historical Mining Site. *Forests* 12(3), 355.

881 Tapia, J., Murray, J., Ormachea, M., Tirado, N., Nordstrom, D. K., 2019. Origin, distribution, and
882 geochemistry of arsenic in the Altiplano-Puna plateau of Argentina, Bolivia, Chile, and Perú. *Sci.*
883 *Total Environ.* 678, 309-325.

884 Tiankao, W., Chotpantararat, S., 2018. Risk assessment of arsenic from contaminated soils to shallow
885 groundwater in Ong Phra Sub-District, Suphan Buri Province, Thailand. *J. Hydro. Regional Stud.*
886 19, 80-96.

887 Ungureanu, G., Santos, S., Boaventura, R., Botelho, C., 2015. Arsenic and antimony in water and
888 wastewater: overview of removal techniques with special reference to latest advances in
889 adsorption. *J. Environ. Manage.* 151, 326-342.

890 Varsányi, I. Kovács, L. O., 2006. Arsenic, iron and organic matter in sediments and groundwater in
891 the Pannonian Basin, Hungary. *Appl. Geochem.* 21, 949-963.

892 Violante, A., Pigna, M., 2002. Competitive sorption of arsenate and phosphate on different clay
893 minerals and soils. *Soil Sci. Soc. Am.* 66, 1788-1796.

894 Wan, X., Li, C., Parikh, S.J., 2020. Simultaneous removal of arsenic, cadmium, and lead from soil by
895 iron-modified magnetic biochar. *Environ. Pollut.* 261, 114157.

896 Wang, J., Xu, J., Xia, J., Wu, F., Zhang, Y., 2018. A kinetic study of concurrent arsenic adsorption
897 and phosphorus release during sediment resuspension. *Chem. Geol.* 495, 67-75.

898 Wang, S., Mulligan, C.N., 2006a. Effect of natural organic matter on arsenic release from soils and
899 sediments into groundwater. *Environ. Geochem. Health* 28, 197-214.

900 Wang, S., Mulligan, C.N., 2006b. Natural attenuation processes for remediation of arsenic
901 contaminated soils and groundwater. *J. Hazard. Mater.* 138, 459-470.

902 Welch, A.H., Stollenwerk, K.G., 2003. Arsenic in ground water: geochemistry and occurrence,
903 Springer Science & Business Media.

904 Wenzel, W.W., Brandstetter, A., Wutte, H., Lombi, E., Prohaska, T., Stingeder, G., Adriano, D.C.,
905 2002. Arsenic in field-collected soil solutions and extracts of contaminated soils and its
906 implication to soil standards. *J. Plant Nut. Soil Sci.* 165(2), 221-228.

907 Williams, L.E., Barnett, M.O., Kramer, T.A., Melville, J.G., 2003. Adsorption and transport of
908 arsenic(V) in experimental subsurface systems. *J. Environ. Qual.* 32(3), 841-850.

909 Wilson, S.C., Lockwood, P.V., Ashley, P.M., Tighe, M., 2010. The chemistry and behaviour of
910 antimony in the soil environment with comparisons to arsenic: a critical review. *Environ. Pollut.*
911 158(5), 1169-1181.

912 Xie, Z., Wang, J., Wei, X., Li, F., Chen, M., Wang, J., Gao, B., 2018. Interactions between arsenic
913 adsorption/desorption and indigenous bacterial activity in shallow high arsenic aquifer sediments
914 from the Jiangnan Plain, Central China. *Sci. Total Environ.* 644, 382-388.

915 Xie, Z., Zhou, Y., Wang, Y., Luo, Y. Sun, X., 2013. Influence of arsenate on lipid peroxidation levels
916 and antioxidant enzyme activities in *Bacillus cereus* strain XZM002 isolated from high arsenic
917 aquifer sediments. *Geomicrobiol. J.* 30, 645-652.

918 Yang, J.K., Barnett, M.O., Jardine, P.M., Basta, N.T., Casteel, S.W., 2002. Adsorption, sequestration,
919 and bioaccessibility of As(V) in soils. *Environ. Sci. Technol.* 36(21), 4562-4569.

920 Yolcubal, I., Akyol, N.H., 2008. Adsorption and transport of arsenate in carbonate-rich soils: Coupled
921 effects of nonlinear and rate-limited sorption. *Chemosphere* 73(8), 1300-1307.

- 922 Zeng, X., Wu, P., Su, S., Bai, L., Feng, Q., 2012. Phosphate has a differential influence on arsenate
923 adsorption by soils with different properties. *Plant Soil Environ.* 58(9), 405-411.
- 924 Zhang, H., Yuan, H., Hu, Y., Wu, Z., Zhu, L.A., Zhu, L., Li, F.B., Li, D., 2006. Spatial distribution
925 and vertical variation of arsenic in Guangdong soil profiles, China. *Environ. Pollut.* 144(2), 492-
926 499.
- 927 Zhang, H., Selim, H., 2005. Kinetics of arsenate adsorption - desorption in soils. *Environ. Sci.*
928 *Technol.* 39(16), 6101-6108.
- 929 Zhang, W., Singh, P., Paling, E., Delides, S., 2004. Arsenic removal from contaminated water by
930 natural iron ores. *Miner. Eng.* 17, 517-524.
- 931 Zhou, J.L., Siddiqui, E., Ngo, H.H., Guo, W., 2014. Estimation of uncertainty in the sampling and
932 analysis of polychlorinated biphenyls and polycyclic aromatic hydrocarbons from contaminated
933 soil in Brighton, UK. *Sci. Total Environ.* 497-498, 163-171.